11

Negative Feedback Semiconductor Optical Amplifiers and All-Optical Triode

Yoshinobu Maeda
Kinki University
Japan

1. Introduction

The field of optical communications is moving toward the realization of photonic networks with wavelength division multiplexing (WDM) utilizing the full bandwidth of optical fibers. Conventionally, an erbium-doped fiber amplifier (EDFA) and a semiconductor optical amplifier (SOA) are used for amplifying an optical signal in optical communications. SOAs can contribute to this and offer the key advantages of small size and ease of mass production, but their practical adoption has been largely precluded by their inferior polarization dependence and noise characteristics as compared those of with optical fiber amplifiers doped with erbium and other rare earths. For eliminating noise generated in such amplifiers, the optical signal that is transmitted at a high speed is once converted into an electrical signal, so as to be subjected to noise elimination and signal processing in an electronic circuit, and the processed signal is then reconverted into an optical signal to be transmitted. This incapability to achieve direct processing of an optical signal without its conversion into an electrical signal limits the speed of the optical signal processing. Therefore, there has been demanded a technique which enables an optical signal to be processed without its conversion into an electrical signal. However, in a field of optoelectronics, there have not yet realized high-performance signal amplifiers corresponding to a negative feedback amplifier or an operational amplifier known in a field of electronics. The negative feedback amplifier in electronics is capable of providing an output signal whose gain, waveform and baseline are stabilized without generating large noise. Negative feedback amplification is widely used in electronics and readily enables gain stability and low-noise electric signal amplification, as the existence of negative- and positive- valued entities facilitate its design and implementation. For optical signals, however, the absence of negative-valued entities poses the need for special techniques. One technique for SOA gain stabilization which has been the subject of research and development at many institutions is the use of a clamped-gain SOA (Bachmann et al., 1996), which utilizes a lasing mode generated outside the signal band. An SOA with gain control obtained by an experimental feedback loop system utilizing a bandpass filter (Qureshi et al., 2007), which is conceptually similar to the technique we have proposed, has also been reported (Maeda, 2006).

In the present study, we utilized phase mask interferometry to fabricate an optical fiber filter (a fiber Bragg grating; FBG) having reflection wavelength characteristics specially designed for surrounding light feedback, formed a lens in the optical fiber tip, and coupled the fiber

containing the FBG to the SOA, thus constructing a "negative feedback SOA (NF-SOA)", and performed measurements of its bit error rate (BER) in correspondence with the input signal, its noise figure, and other characteristics, which show its noise reduction effect (Maeda et al., 2010).

In previous study, it has been demonstrated that an all-optical triode can be achieved using a tandem wavelength converter employing cross-gain modulation (XGM) in SOAs (Maeda et al., 2003). Basic functions such as switching can be achieved using all optical gates realized by optical nonlinearities in semiconductor materials (Stubkjaer, 2000). The three mainly used schemes to perform their wavelength conversion employing SOAs are based on XGM, cross-phase modulation (XPM), and four-wave mixing (FWM) (Glance et al., 1992; Durhuus et al., 1994; Wiesenfeld, 1996). The XGM scheme has the advantage to be very simple: an input modulated signal and a continuous-wave beam are introduced into the SOA. The input signal saturates the SOA gain and modulates the cw beam inversely at the new wavelength. A large signal dynamic theoretical model was presented for wavelength conversion using XGM in SOA with converted signal feedback (Sun, 2003). The theoretical results predict that the wavelength conversion characteristics can be enhanced significantly with converted signal feedback. We demonstrated a negative feedback optical amplification effect that is capable of providing an output signal whose gain and waveform are stabilized optically using XGM in SOA with amplified spontaneous emission feedback (Maeda, 2006). We have also previously proposed a tandem wavelength converter in the form of an all-optical triode with cross-gain modulation (XGM) in two reflective semiconductor amplifiers (RSOAs), and demonstrated the signal amplifying effect of its three terminals (Maeda et al., 2003). In investigating the cause of an increase in extinction ratio found in the XGM of the RSOAs, we were able to elucidate the negative feedback optical amplification effect and its potential for SOA noise reduction. This effect is due to the feedback to the SOA of spontaneous emission generated in the SOA in response to the input light signal. The spontaneous emission is intensity inverted with respect to the input light signal effected by XGM in the SOA. It can thus be used to dynamically modulate the SOA internal gain in correspondence with the input optical signal, and achieve a noise reducing effect analogous to that of electronic negative feedback amplification.

2. Negative feedback optical amplification effect

Fig. 1 shows the block diagram of the negative feedback optical amplifier. It consists of a semiconductor optical amplifier and an optical add/drop filter, which is equipped with a negative feedback function. It is used the SOA based on ridge waveguide structure InGaAsP/InP MQW material. The composition of the InGaAsP active layer is chosen to have a gain peak wavelength around 1550 nm. The maximum small signal fiber-to-fiber gain is around 15 dB and the output saturation power is approximately 2 mW measured at 1550 nm with a bias current of 250 mA. A tunable laser is used for the input signal, which is modulated by the mean of electro-optic modulators connected to an electrical synthesizer. The input signal is the wavelength of 1550 nm. The modulated input signal is fed into the SOA using an optical coupler. An add/drop filter (spectral half-width: 13 nm) is set at the center wavelength of 1550 nm. The filter is provided to extract an output signal light of the wavelength of 1550 nm and surrounding spontaneous emission L_S having wavelengths (L_S <1543.5 and L_S >1556.5 nm) other than 1550±6.5 nm. Because of the XGM mechanism in the SOA, the spontaneous emission L_s contain an inverted replica of the information carried by

the input signal. The output of L_s is fed back and injected together with the input signal into the SOA by using an optical coupler. A variable optical attenuator (VOA) is provided in an optical feedback path. The average output power is measured at the output of the filter using an optical power-meter.

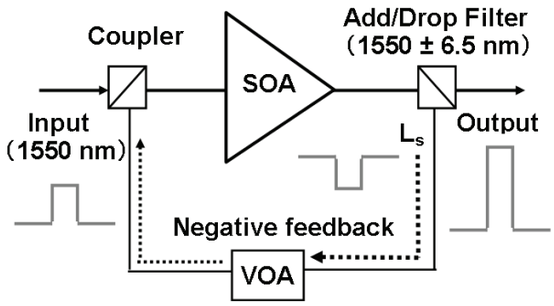

Fig. 1. Block diagram of a negative-feedback semiconductor optical amplifier. VOA: Variable optical attenator.

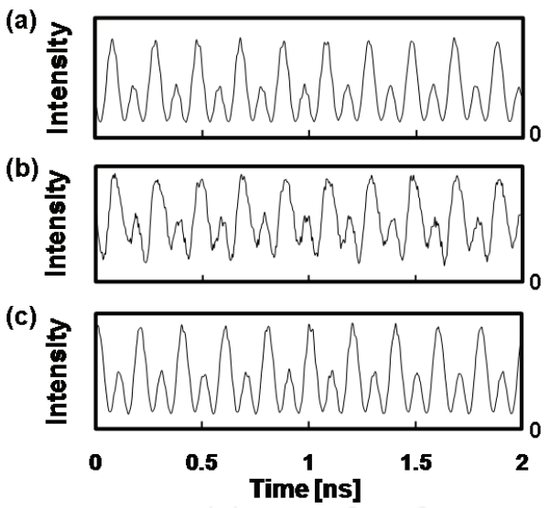

Fig. 2. (a) Input waveform, (b) and (c) Output waveform without and with negative feedback, respectively.

Figs. 2(a), 2(b) and 2(c) show waveforms of the input, the output without negative feedback and the output with negative feedback, respectively. The input average power is approximately 2 mW. They have been measured with a fast photodiode connected to a sampling head oscilloscope. The modulation degree and frequency of the input continuous signal are 80% and 10 GHz, respectively. The modulation degree M is equal to $100 \times (P_{max} - P_{min})/(P_{max} + P_{min})$ [%], where P_{max} and P_{min} represent the maximum and minimum intensities of the signal, respectively. As is apparent from Figs. 2(b) and 2(c), the output signal was given a higher modulation degree M, a waveform with a higher fidelity and a more stable baseline in the case where the SOA feeding back the spontaneous emission L_s was used with negative feedback, than in the case where the SOA was used without negative feedback. The output average power was around 6.4 mW without negative feedback, as shown in Fig. 2(b). On the other hand, in the SOA with negative feedback, the

output average power was approximately 1.9 mW when the negative feedback average power was 0.12 mW, as shown in Fig. 2(c). Therefore, the output signal waveform with negative feedback is remarkably improved over that without negative feedback. Moreover, in the SOA with negative feedback, the distortion of the waveform is extremely small in a wide frequency band of 0.1 – 10 GHz.

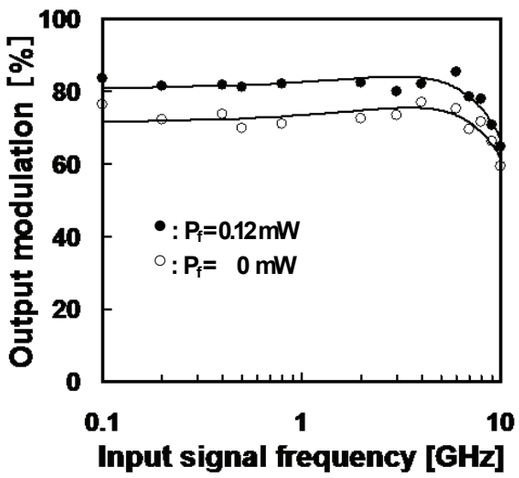

Fig.3. Relationship between the output modulation degrees and the frequency of the input signal.

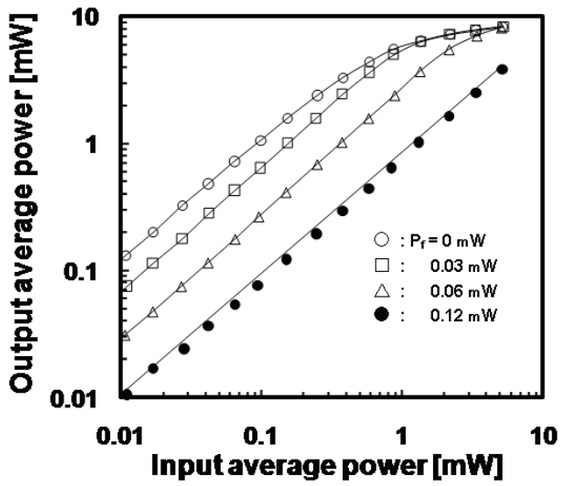

Fig. 4. Relationship between the output average and input average powers for four values of the negative feedback average powers (P_f = 0, 0.03, 0.06, 0.12 mW).

Fig.3 shows the relationship between the output modulation degrees and the frequency of the input signal. The input modulation degree depends on the input signal frequency and decreases relatively at higher frequency due to the characteristics of the electro-optic modulator. The average power of input signal is around 2 mW. The black-dot (●) represents the case of the SOA when the negative feedback average power was around 0.12

mW and the white-dot (○) represents without negative feedback. The output modulation degree (i.e., extinction ratio) with negative feedback is remarkably improved over that without negative feedback in a wide input signal frequency band of 0.1-10 GHz.

Fig. 4 shows the relationship between the output average and input average powers for four values of the negative feedback average powers (P_f = 0, 0.03, 0.06, 0.12 mW). The modulation degree and frequency of the input signal are around 100% and 0.1 GHz, respectively. The input-output characteristic in the SOA with negative feedback has a higher linearity than that without negative feedback. It is also noted that a gain G is defined as $G = 10 \log_{10} (P_{out}/P_{in})$ [dB], where P_{out} and P_{in} represent the respective output and input signal power.

Fig. 5 shows the gain characteristic, i.e., a relationship between the gain and the input signal average power. The gain G with negative feedback is found to be lower than that without negative feedback when the negative feedback average power increases from 0 to 0.12 mW. For P_f = 0.12 mW, the gain remains approximately 0 dB for input signal average powers between 0.01 to 5 mW. In addition, the gain can be adjusted optically between 0 and 11 dB by changing the amount of negative feedback using a variable optical attenuator.

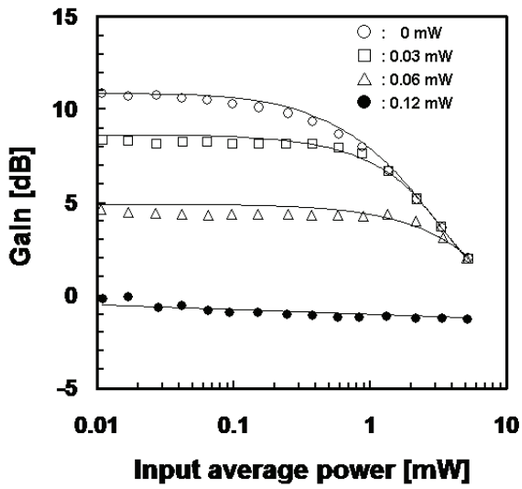

Fig. 5. Relationship between the gain and the input signal average power for four values of the negative feedback average powers (P_f = 0, 0.03, 0.06, 0.12 mW).

In general, since a conventional optical amplifier merely has a simple amplification function (that is almost constant gain), the amplifier disadvantageously amplifies not only the signal but also the noise. Therefore, the waveform and baseline of the output signal cannot be improved basically in relation with the noise, thereby making difficult to achieve an advanced signal processing. For eliminating noise generated in such amplifiers, the optical signal is once converted into an electrical signal, so as to be subjected to noise elimination and signal processing in an electronic circuit, and the processed signal is then reconverted into an optical signal to be transmitted. Fig. 6 shows the concept diagram of a negative feedback optical amplification effect. Figs. 6(a), 6(b) and 6(c) show waveforms of the input, the negative feedback and the gain in SOA, respectively. In the SOA which has a XGM function, spontaneous emission lights which have wavelengths near a wavelength λ_1 of an input light have an intensity varying in response to a variation in the intensity of that input light. Characteristically, the intensity variation of the spontaneous emission lights are

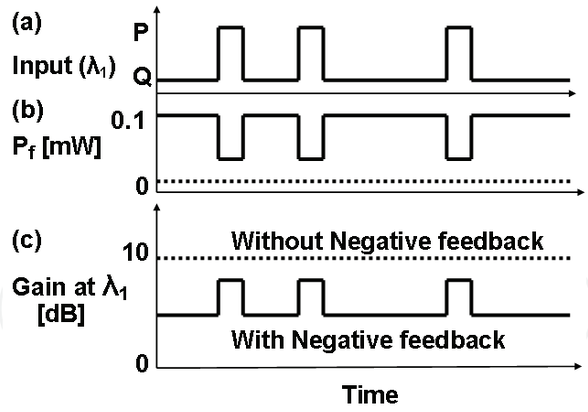

Fig. 6. Concept diagram of a negative feedback optical amplification effect. The straight-line represents the case where the SOA was used with negative feedback, and the dotted line represents the case of the SOA without negative feedback.

inverted with respect to the variation in the input signal, and the spontaneous emission lights are outputted from the SOA, as shown in Fig. 6(b). The straight-line represents the case where the SOA was used with negative feedback, and the dotted line represents the case of the SOA without negative feedback. In the past, it is common that the spontaneous emission lights as the surrounding light having wavelengths other than the wavelength λ_1 are removed by a band-pass filter, since it becomes a factor of noise generation. In such a situation, we found out that a negative feedback optical signal amplification phenomenon in which characteristics of the gain of the SOA is drastically changed by feeding back the separated surrounding light to the SOA, so that the gain is modulated as shown in Fig. 6(c). Therefore, noise reduction is realized all-optically in the SOA, because the output signal waveform with negative feedback is remarkably improved over that without negative feedback, as shown in Fig. 2. Moreover, the baseline of the output signal waveform is suppressed, because the gain in the SOA is low when the power of the input signal is at the low logical level, whereas the output signal is stressed because of the high SOA gain when the input signal power is high, as shown in Fig. 6. In addition, the desired gain was set between 0 and 11 dB by changing the amount of the negative feedback, as shown in Fig. 4. The negative feedback optical amplifier is capable of providing an output signal whose gain is stabilized automatically.

An operational amplifier of the field of electronics has two inputs consisting of a non-inverse input and an inverse input, and is used as a negative feedback circuit for feeding a part of an output voltage of an amplifier, back to the inputs through an external resistance. The operational amplifier is referred to as a non-inverting amplifier where an output is in phase with an input, and is referred to as an inverting amplifier where the phase of the output is delayed by π. The optical amplifier of the present work is physically considered as the optical equivalent of a non-inverting amplifier, since the output is in phase with the input. In addition, the non-inverting amplifier of the electronics is provided a voltage gain of not lower than 1, the gain is 0 dB where the resistance in the feedback path is 0, namely, where the feedback path is provided by a short circuit. The operational amplifier is capable of achieving an analog computing such as summing, differentiating and integrating amplifier. It is therefore no exaggeration to say that the operational amplifier takes change of a major part of an analog electronic circuit today. The optical amplifier of the present

work can take charge of an important role in an optical circuit, as the negative feedback or operational amplifiers in electronics.
Therefore, we found out that the negative feedback optical amplification effect is capable of providing an output signal whose gain, waveform and baseline are stabilized automatically. The optical amplifier consists of an InGaAsP/InP semiconductor optical amplifier and an optical add/drop filter, which is equipped with a negative feedback function. In the SOA with negative feedback, the output modulation degree was substantially higher modulation degree and the distortion of the waveform was extremely small in wide frequency band of 0.1 – 10 GHz. The gain in the SOA with negative feedback is suppressed to be lower than that without negative feedback and reaches around 0 dB when the negative feedback power increases. In addition, the desired gain was set between 0 and 11 dB by changing the amount of the negative feedback. The optical amplifier is physically considered as the optical equivalent of a non-inverting amplifier, since the output is in phase with the input. Therefore, the negative feedback optical amplifier of this work can take charge of an important role in an optical circuit, as the negative feedback amplifier in electronics.

3. Negative feedback optical semiconductor amplifier

3.1 Fiber Bragg gratings based on phase mask interferometer

The fiber Bragg grating (FBG) used in the present study is a diffraction grating formed inside an optical fiber. Bragg diffraction gratings are characterized by their reflection of light of certain wavelengths. The FBG is a refractive index modulation grating, with alternating regions of high and low refractive indices in the direction of light propagation. The relation between the grating period Λ and the reflection wavelength (the Bragg wavelength) λ_B is expressed as

$$\lambda_B = 2n_{eff}\Lambda \tag{1}$$

n_{eff} : effective refractive index. The refractive index of the core is raised above that of the clad by adding GeO_2, which induces oxygen-deficient defects in the SiO_2 with an absorption band in the vicinity of 240 nm. A rise in the refractive index occurs under UV irradiation in that vicinity. This has been variously attributed to the Kramers-Kroning relation (the relation between light absorption and change in refractive index) and to the occurrence of defects in the glass structure due to molecular reorientation under UV irradiation. It has also been reported that UV sensitivity can be substantially heightened by pre-treatment with high-pressure hydrogen. In the present study, the change in the optical refractive index was utilized to obtain refractive index modulation in the fiber core as shown in Fig.7.

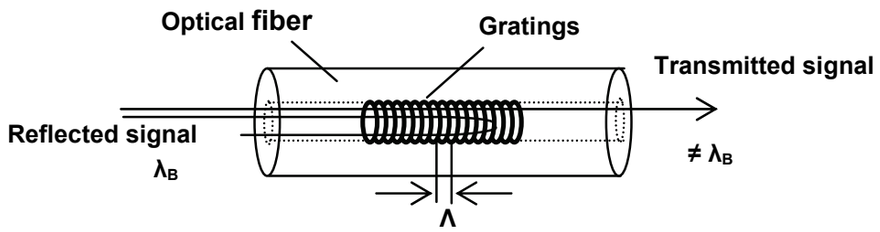

Fig. 7. Drawing of the fiber Bragg grating. Λ : grating period, λ_B : Bragg wavelength.

Phase mask processing is a widely used technique for optical device fabrication. After removal of its covering, the fiber is irradiated from the side (in the circumferential direction) by an intense UV laser beam, which is diffracted by the phase mask and thus forms an interference pattern in the fiber core, resulting in the formation of a refractive index modulation pattern in the core corresponding to the period of the interference pattern. The grating period Λ in the core is 1/2 of the phase mask grating period d, with good reproducibility. A key advantage of the phase mask technique is that it enables the use of a low-coherence laser beam. An alternative technique for the same purpose is the two-light-bundle interference light exposure method. Although it is relatively low in reproducibility, it may be advantageous for multi-grade low-volume production, as it requires no phase mask, which is an expensive consumable, and it enables the use of a broad range of wavelengths in the same optical system. For the production of a chirp grating, however, in which the grating period is gradually changed and the reflection wavelength band is thus broadened, it requires the incorporation of lens systems into the interferometer and presents difficulties relating to adjustment.

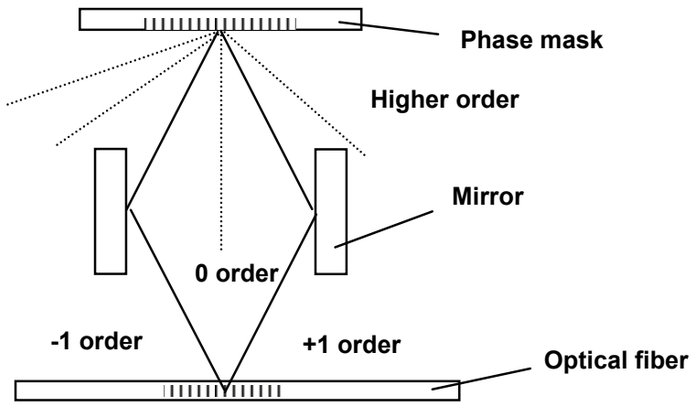

Fig. 8. Phase mask interferometer. The +/− primary light refracted by the phase mask is returned by the mirror.

In the present study, we used the phase mask interference method shown schematically in Fig. 8 as the production/fabrication process. It combines the high reproducibility of the phase mask method and the broad wavelength response of the two-beam interference technique. Only the +/− primary light refracted by the phase mask is returned by the mirror, and the interference fringe period can be controlled by adjusting its angle. It is therefore possible to prevent interference with higher-order diffraction light, and thus reduce passband loss. The key functions required in the fiber grating filter include transmission at the wavelength of the light input to the SOA and feedback to the SOA of a part of the surrounding light generated during amplification. We therefore fabricated the FBG with the transmission and reflection spectra shown in Fig. 9, and with a 92% reflectance ratio. The surrounding light has a certain fixed spread, and it is necessary to provide a spread in the reflection band of the fiber grating. For this purpose, two chirp gratings with slightly different reflection center wavelengths (1548 and 1554 nm) were written in mutually close proximity on the optical fiber. The use of the phase mask interference technique facilitated the selection and control of the reflection center wavelengths, adjustment of the

writing positions on the fiber, and other aspects. High stability and reproducibility in the FBG fabrication were also ensured through the use of an original adjustment algorithm and computerized control of the optical system for optical fiber position and mirror angle, unlike the conventional processes which usually depend on visual methods. The tip of the prototype FBG was lensed and coupled to one end of the SOA, thus obtaining a negative-feedback semiconductor optical amplifier (NF-SOA).

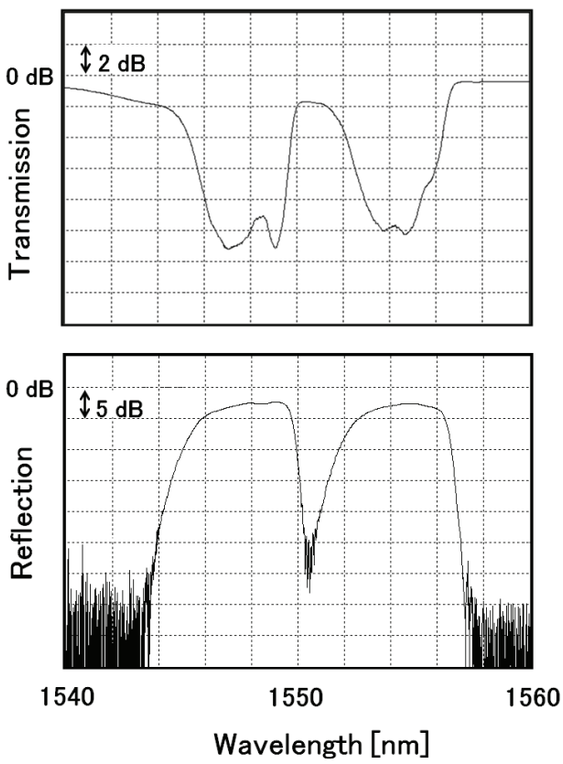

Fig. 9. Transmission and reflection spectrum of the fiber Bragg grating for negative feedback optical amplifier.

3.2 Measurement results of NF-SOA

The composition of the NF-SOA and the measurement system is shown schematically in Fig. 10. The SOA was an InGaAsP-InP ridge semiconductor optical amplifier. The center wavelength of the InGaAsP multi-quantum-well active layer was approximately 1500 nm and the gain at the fiber end was approximately 17 dB with a 250 mA electric current input. As shown by the saturation gain curve in Fig. 11 with the 1550-nm input signal, the gain was constant in the light output power range of −25 to 0 dBm and the saturation power was 7 dBm. Fig. 12 shows the spectrum of the amplified spontaneous emission (ASE) of the SOA, with the characteristics shown in Fig. 9 for the FBG mounted at the output end of the SOA clearly evident in the vicinity of 1550 nm. In the measurement system, the intensity of the wavelength-tunable laser beam was modulated by a lithium niobate (LN) optical modulator. After amplification of the signal by an Er-doped optical fiber amplifier (EDFA), it was passed through a 1-nm bandwidth-tunable filter, and its intensity was then modulated by a variable optical attenuator (VOA) to obtain the input signal. To experimentally verify that it

is possible to reduce the output light waveform distortion as an effect of the negative feedback optical amplification, we measured the bit error rate in the transmission of random bits used in optical communication, using an Anritsu PM-1800 signal quality analyzer. The pattern generator provided a continuous signal with an NRZ 2^{31}-1 pseudorandom bit sequence at 10 Gbps.

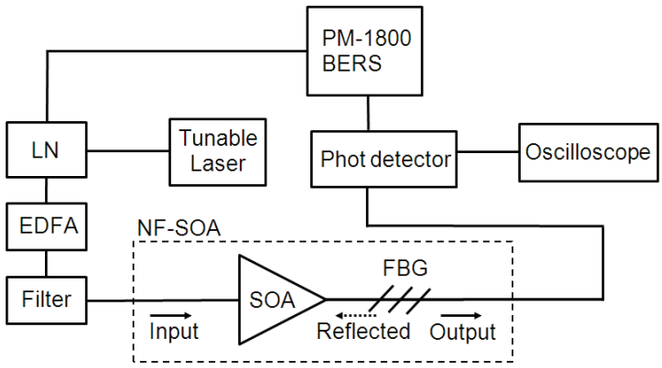

Fig. 10. Block diagram of the negative feedback semiconductor optical amplifier (NF-SOA) and measurement system.

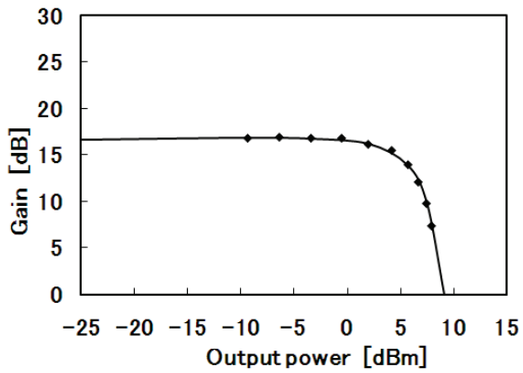

Fig. 11. Characteristic of saturation gain curve for NF-SOA.

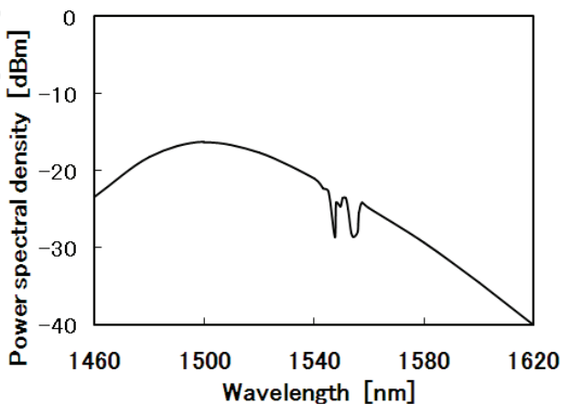

Fig. 12. Amplified spontaneous emission (ASE) spectrum for NF-SOA.

Fig. 13 shows eye-pattern waveforms observed on the oscilloscope, for output light with (a) NF-SOA and (b) SOA, respectively. Figs. 14(a)-14(d) show the eye-pattern waveforms observed on the oscilloscope, for output light with NF-SOA input signals (−7 dBm) at laser beam wavelength settings of 1530, 1544, 1550, and 1558 nm, respectively.

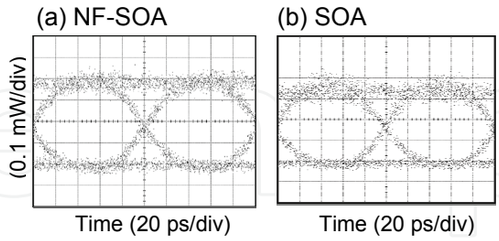

Fig. 13. Eye-pattern waveforms of (a) NF-SOA and (b) SOA at 1550 nm.

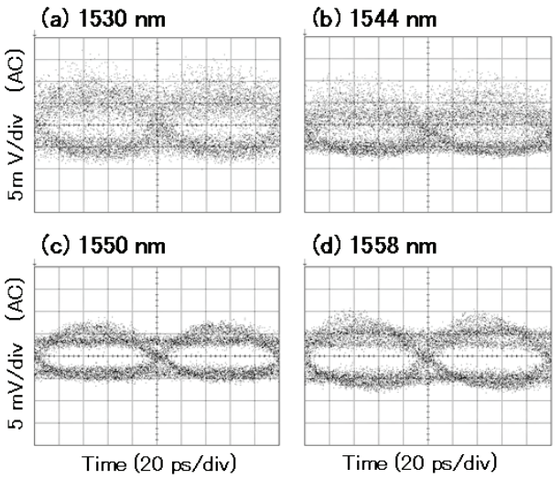

Fig. 14. Eye-pattern waveforms of (a) 1530, (b) 1544, (c) 1550 and (d) 1558 nm for NF-SOA.

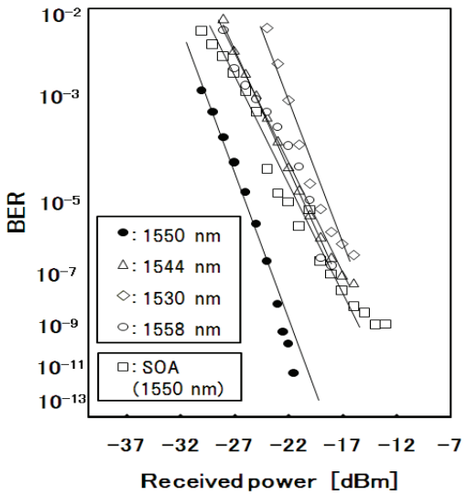

Fig. 15. Measured BER results for the NF-SOA. 1530 (●), 1544 (△), 1550 (◊), and 1558 (○) nm.

The observed aperture ratios were (a) 0.35, (b) 0.37, (c) 0.50, and (d) 0.41, and the waveform at the FBG transmission center wavelength of 1550 nm, as shown in Fig. 14(c), thus exhibited an eye pattern with a better aperture ratio than the other waveforms. Fig. 15 shows the BER measurements for the NF-SOA with laser settings of 1530 nm (●), 1544 nm (△), 1550 nm (◊), and 1558 (○) nm. As shown by the BER curves, the 1550-nm wavelength resulted in lower BER values than the other wavelengths at the same received power and a power penalty of approximately 1 dB or more. For reference, the measured BER values for the conventional SOA at an optical input wavelength of 1550 nm (□) are also shown. These BER curves demonstrate that the NF-SOA provides lower BER values than the SOA at 1550 nm with the same level of received power. As shown clearly in Fig. 15, the NF-SOA BER curve at 1550 nm achieves a higher negative power penalty than the curve without NF. This indicates that an NF-SOA module can reduce the bit error rate more than an SOA module without NF when random optical signals are transmitted.

Wavelength	G_{max}	G_{min}	PDG	NF
1530 nm	18.3 dB	17.7 dB	0.62 dB	8.3 dB
1544 nm	16.8 dB	16.2 dB	0.63 dB	6.1 dB
1550 nm	17.1 dB	16.0 dB	0.68 dB	5.1 dB
1558 nm	17.2 dB	15.8 dB	0.69 dB	6.2 dB

Table 1. Specification of gain, polarization dependent gain, and noize figure for NF-SOA.

Wavelength	G_{max}	G_{min}	PDG	NF
1530 nm	24.8 dB	24.1 dB	0.78 dB	9.3 dB
1544 nm	22.9 dB	22.7 dB	0.70 dB	8.9 dB
1550 nm	22.0 dB	21.5 dB	0.75 dB	9.0 dB
1558 nm	20.9 dB	20.1 dB	0.76 dB	9.1 dB

Table 2. Specification of gain, polarization dependent gain, and noize figure for SOA.

The characteristics of the NF-SOA and SOA are summarized in Tables 1 and 2, respectively, in terms of maximum and minimum gain (G_{max} and G_{min}), polarization dependent gain (PDG), and noize figure (NF). PDG, the gain of the optical amplifier dependent on the polarization state of the input light signal, is generally low in high-performance amplifiers. The PDG was determined by Muller's method, and the NF was calculated from the S/N ratio of the optical signal (OSNR). As shown by comparison of Tables 1 and 2, the feedback by the FBG of part of the spontaneous emission resulted in a somewhat smaller gain with the NF-SOA than that obtained with the conventional SOA. The NF values of 8.3 dB at 1530 nm, 6.1 dB at 1544 nm, and 6.2 dB at 1558 nm, and particularly 5.1 dB at the FBG transmission center wavelength of 1550 nm obtained with the NF-SOA, however, were all smaller that the value of approximately 9 dB obtained with the conventional SOA at all of these wavelengths, thus clearly demonstrating the noise reduction effect of the negative feedback optical amplification. The PDG values of the NF-SOA (Table 1), moreover, were all approximately 0.1 dB smaller than those of the conventional SOA (Table 2) at all wavelengths, further demonstrating its low polarization dependence and excellent characteristics.

4. All-optical triode

4.1 All-Optical Triode Based on NF-SOA

Fig. 16 shows the block diagram of the optical triode. It consists of two cascaded wavelength converters based on two NF-SOAs. Two tunable lasers are used for the input and the control signals, which are modulated by the mean of electro-optic modulators connected to an electrical synthesizer and a pattern generator respectively. Both input and control signals have the same wavelength equal to 1551 nm. The modulated input signal is fed into the first SOA (SOA-1) using an optical Add/drop filter (central wavelength: 1551 nm, spectral half-width: 0.8 nm). Because of the XGM mechanism in the SOA-1, the FBG-1 reflection beam (Ls) contains an inverted replica of the information carried by the input signal. The modulated output Ls is then injected together with the control signal into the second SOA (SOA-2) by using an optical coupler. A band pass filter (spectral half-width: 0.8 nm) of the central wavelength equal to 1551 nm is placed after the SOA-2. The average output power is measured at the output of the filter. In the second wavelength conversion stage the Ls beam is converted back to the 1551 nm wavelength depending on the power of the control beam.

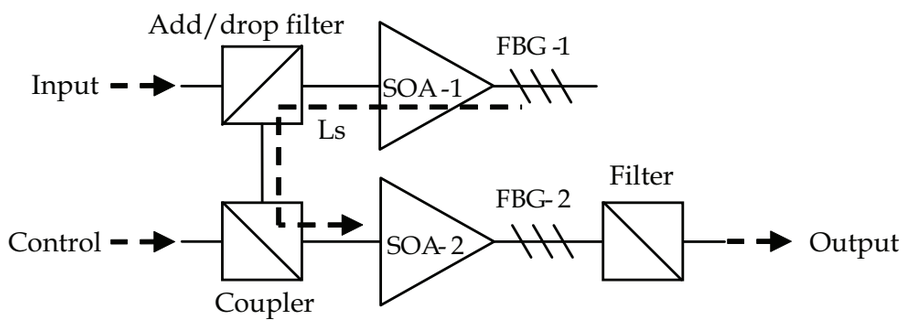

Fig. 16. Block diagram of the all-optical triode. SOA-1 and SOA-2: Semiconductor optical amplifier, FBG-1 and FBG-2: Fiber Bragg grating.

Figs. 17(a) and 17(b) show the input and control signal waveforms, respectively. They have been measured with a fast photodiode connected to a sampling head oscilloscope. The modulation degree and frequency of the input signal are 90% and 1 GHz, respectively. The modulation degree M is equal to $100 \times (P_{max} - P_{min})/(P_{max} + P_{min})$ [%], where P_{max} and P_{min} represent the maximum and minimum intensities of the signal, respectively. Fig. 17(c) shows the output waveforms for four values of the control average power P_c. The information of the input signal is transmitted to the output only when the power of the control signal is at the high logical level, whereas it is blocked when the control power is low. The magnitude of the output waveform is controlled by the power of the control beam: the larger P_c, the higher the peak power at the output.

Fig. 18 shows the dependence of the output power (P_{out}) on the input power (P_{in}) for four values of the control power (P_c). It can be seen that the output power increases when the control power is increased. Fig. 19 shows the dependence of the modulation degree of the output signal on the input signal frequency. By increasing the input signal frequency from 0.1 to 10 GHz, the modulation degree M decreases from 60% to 0%. For frequencies smaller than 2 GHz, M remains approximately the same as the input modulation degree.

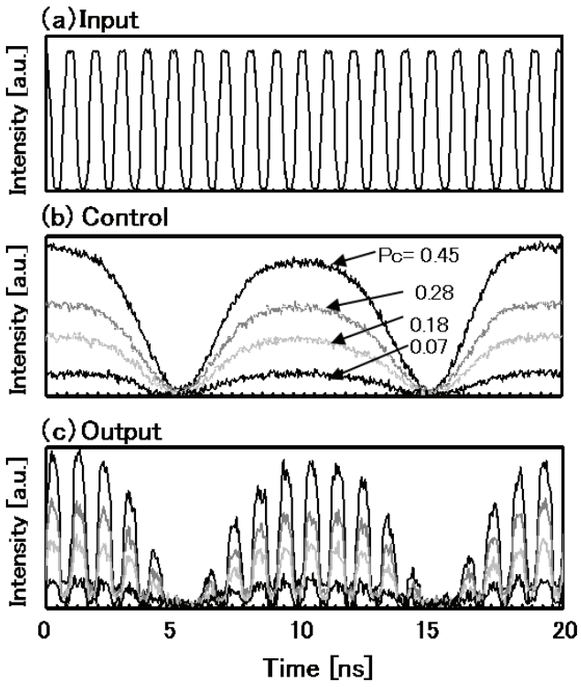

Fig. 17. (a) Input and (b) control signal waveforms. (c) Output waveforms for four values of control average power (Pc=0.45, 0.28, 0.18, 0.07).

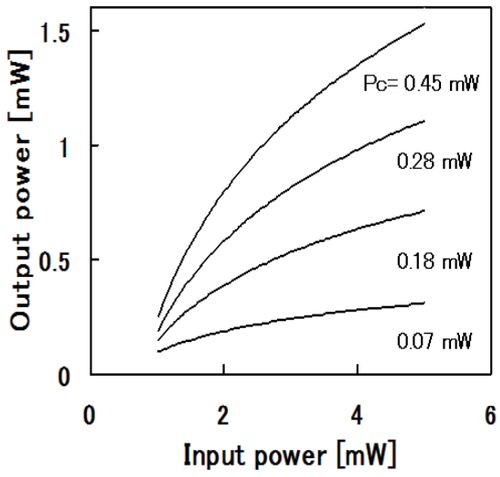

Fig. 18. Output versus input power four for values of the control average power (Pc=0.45, 0.28, 0.18, 0.07).

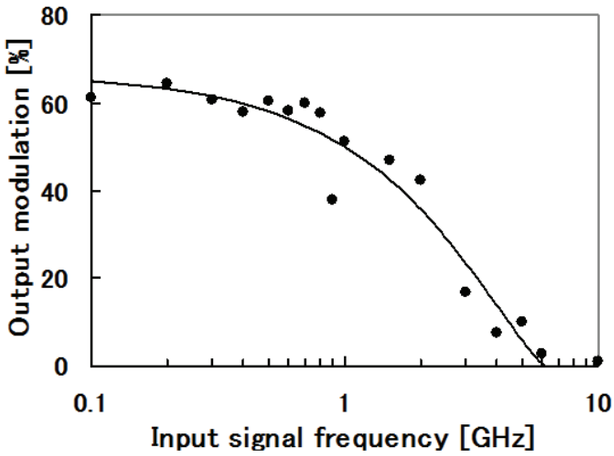

Fig. 19. Output modulation degree versus input signal frequency.

4.2 All-Optical Triode using reflective semiconductor optical amplifiers

Fig. 20 shows the block diagram of the optical triode. It consists of two cascaded wavelength converters based on two RSOAs, which are similar to standard SOAs with one of the facets high-reflection coated. We used two RSOAs based on ridge waveguide structure InGaAsP/InP bulk material. The composition of the InGaAsP active layer is chosen to have a gain peak wavelength around 1555 nm. The small signal fiber-to-fiber gain is around 20 dB and the output saturation power is approximately 2 mW measured at 1555 nm with a bias current of 250 mA. Two tunable lasers are used for the input and the control signals, which are modulated by the mean of electro-optic modulators connected to an electrical synthesizer and a pattern generator respectively. Both input and control signals have the same wavelength equal to 1555 nm. A conventional distributed feedback laser diode is used as bias laser. Its power measured at the point a in Fig. 20 is 0.89 mW (P_b) and the wavelength is 1548 nm. The modulated input signal and the bias beam are fed into the first RSOA (RSOA-1) using an optical coupler and a circulator (C1). The polarization state of both beams is set by maximizing the modulation degree of the bias beam at the RSOA-1 output by using two polarization controllers (P.C.'s).

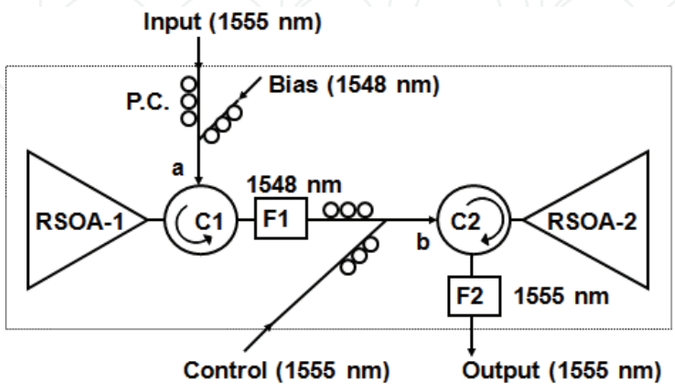

Fig. 20. Block diagram of the optical triode. P.C.: polarization controller, C: circulator, F: tunable band pass filter.

The use of the P.C.'s was necessary because the two employed RSOA are polarization dependent. By using polarization independent devices, the P.C.'s depicted in Fig. 20 are not necessary. A tunable band pass filter at the output of C1 (F1, spectral half-width: 0.6 nm) is set at the center wavelength of 1548 nm to filter away the input signal. Because of the XGM mechanism in the RSOA-1, the bias beam contains an inverted replica of the information carried by the input signal. The modulated output of F1 is then injected together with the control signal into the second RSOA (RSOA-2) by using an optical coupler and a circulator (C2). A second tunable band pass filter (F2, spectral half-width: 1.3 nm) of the central wavelength equal to 1555 nm is placed after the RSOA-2 and it is used to suppress the 1548 nm beam. The average output power is measured at the output of the filter F2. In the second wavelength conversion stage the 1548 nm beam is converted back to the 1555 nm wavelength depending on the power of the control beam.

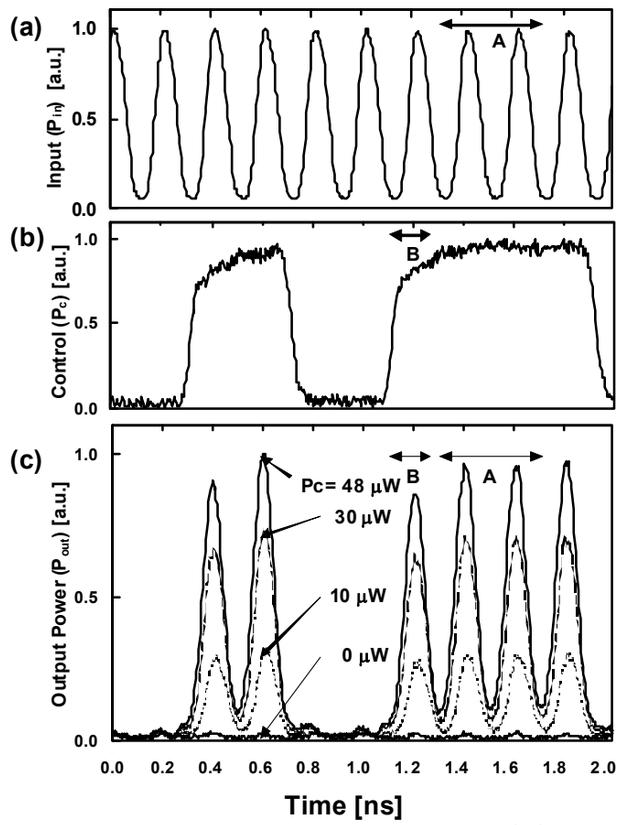

Fig. 21. Input (a) and control (b) signal waveforms. (c) Output waveforms for four values of the control average power (P_c = 0, 10, 30, and 48 μW).

Figs. 21(a) and 21(b) show the input and control signal waveforms, respectively. The average input and control power are 0.86 mW and 48 μW, measured at the points a and b in Fig. 20, respectively. They have been measured with a fast photodiode connected to a sampling head oscilloscope. The modulation degree and frequency of the input signal are 90% and 5 GHz, respectively. The modulation degree M is equal to $100 \times (P_{max} - P_{min})/(P_{max} + P_{min})$ [%], where P_{max} and P_{min} represent the maximum and minimum intensities of the signal, respectively. Fig. 21(c) shows the output waveforms for four values of the control

average power P_c. The information of the input signal is transmitted to the output only when the power of the control signal is at the high logical level, whereas it is blocked when the control power is low. The magnitude of the output waveform is controlled by the power of the control beam: the larger P_c, the higher the peak power at the output. The unequal peak output power between the points A and B in Fig. 21(c) is due to a imperfect shape of the control beam as it is evident from Fig. 21(b). Fig. 22 shows the dependence of the output power (P_{out}) on the input power (P_{in}) for four values of the control power (P_c). These transmission characteristics have been obtained by plotting the data from the marked position A in Figs. 21(a) and 21(c) using the time as parameter. For P_c = 0 μW, the output power is very small, less than 0.1 mW even if the input power varies from 0.2 to 1.8 mW. For the other values of P_c, it can be seen that the output power increases when the control power is increased. If we define the output-input gain parameter g_{tr}= ΔP_{out} /$\Delta P_{in,}$ we obtain values of 0.6, 1.1 and 1.6 for P_c = 10, 30, and 48 μW, respectively, at the input power of 1 mW, whereas g_{tr} is almost equal zero, for P_c = 0. The output-control amplification parameter f, defined as ΔP_{out} /ΔP_c, depends on P_c and P_{in}. For example, when the control peak power increases from 0 to 96 μW, the peak output power increases from 0.1 to 3.3 mW. At the input power of 1.8 mW, f is approximately 33.

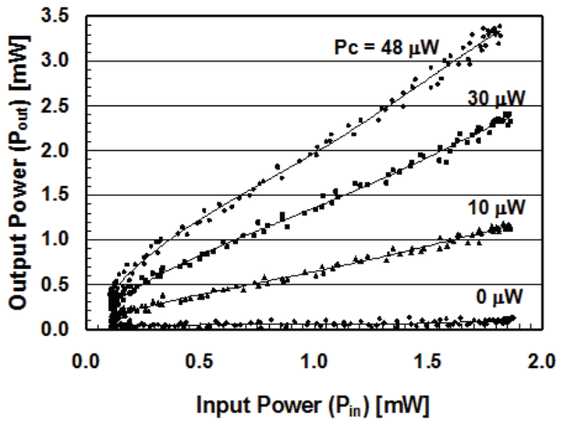

Fig. 22. Output power (P_{out}) versus input power (P_{in}) for four values of the control average power.

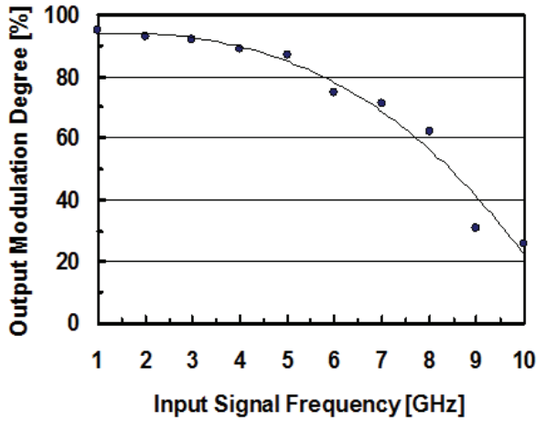

Fig. 23. Output modulation degree versus input signal frequency.

This means that a small change in the control power is able to induce a change 33 times larger at the output. Because of the gain saturation in the SOA, the parameter f decreases when either the input signal power is decreased or the control signal power is increased.
Fig. 23 shows the dependence of the modulation degree of the output signal on the input signal frequency, measured in position marked with A in Fig. 21(c) by using an input modulation degree of approximately 90 %. By increasing the input signal frequency from 1 to 10 GHz, the modulation degree M decreases from 90% to 30%. For frequencies smaller than 5 GHz, M remains approximately the same as the input modulation degree.

5. Discussion

The basic concept of the proposed negative feedback optical amplification effect is shown schematically in Fig. 24.

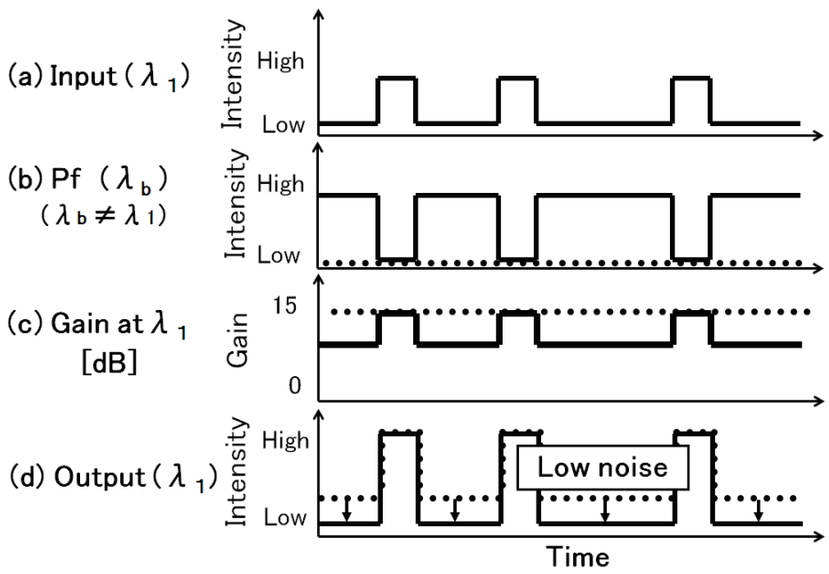

Fig. 24. Concept diagram of a negative feedback optical amplification effect. The straight-line represents the case where the SOA was used with negative feedback, and the dotted line represents the case of the SOA without negative feedback.

When input light of wavelength λ_1 is injected into the SOA as shown in Fig. 24(a), the spontaneous emission at a wavelength λ_b surrounding λ_1, which is generated by the cross-gain modulation within the SOA, undergoes intensity modulation with a reverse phase to that of the input light. This change in intensity is delineated by the solid line in Fig. 24(b). When the resulting $P_f(\lambda_b)$ is fed back to the SOA as negative feedback light, in the cross-gain modulation within the SOA the gain at wavelength λ_1 is modulated as shown by the solid line in Fig. 24(c). In the absence of feedback light P_f, as shown by the dotted line in Fig. 24(c), the SOA gain is constant. In a constant-gain amplifier, the signal and the noise are both amplified with the same gain and it is therefore impossible in principle to increase the signal to noise ratio (S/N ratio). With the negative feedback P_f, in contrast, the gain at wavelength λ_1 is modulated as shown by the solid line in Fig. 24(c). In an SOA with dynamic gain modulation of this nature, with input light injection as shown in Fig. 24(a), the gain is small for input light of low intensity and the degree of amplification is thus low, and the zero level

of the output light is lower than it would be without the negative feedback light P_f. As shown in Fig. 24(d), a high degree of modulation (high extinction ratio) can thus be obtained and it is therefore possible to increase the S/N ratio. Fig. 24 is simply a qualitative illustration of the improvement in the level of output light modulation, but in a previous report (Maeda, 2006), we showed that reduced waveform distortion in the output light and improved modulation can be achieved, as experimentally observed effects of the negative feedback optical amplification.

Positive feedback is performed in optical amplifiers to induce laser oscillation. In electronics, similarly, oscillation tends to occur in an amplifier with positive feedback, and various electronic circuits are utilized as oscillators. Negative feedback is widely used in electronics, as it enables electronic signal amplification with high gain stability and low noise and also makes it possible to stabilize inherently unstable semiconductor elements, for low-noise electric signal amplification. In electronic negative feedback amplification circuits, the degree of amplification is determined by the resistance, which in turn determines the feedback ratio, and effective techniques are essential to avoid temperature dependence in the degree of amplification by transistors, which tend to be highly temperature dependent. In optical amplification, in contrast, the utilization of negative feedback is currently non-existent. For the continuing advance of optoelectronics with optical signals, however, negative feedback optical amplification techniques will presumably be essential. The FBG utilized in the present study is composed primarily of glass, which has a weaker temperature dependence than other semiconductor materials. In negative feedback amplification and other applications, the weak temperature dependence of FBGs in comparison with that of conventional semiconductor SOAs may be expected in principle to facilitate the achievement of systems with increased temperature stability and more specifically the achievement of a superior NF and other optical amplification characteristics through the control of comparatively unstable SOAs by passive FBGs. Detailed experimentation will be required for verification of this possibility.

The improvement of approximately 0.1 dB in PDG observed in the present study with the NF-SOA, as compared with the conventional SOA (Tables 1 and 2), may be attributable to the polarization independent nature of the FBG. As the FBG is not polarization dependent, neither is the light which it returns to the SOA. Although the signal light is not directly influenced by the absence of polarization dependence in the FBG, the influence of polarization on the total SOA gain is presumably reduced by the negative feedback amplification, thus reducing the overall PDG. The data in the present study represents an early stage of experimentation, however, and further data and elucidation will be necessary in relation to the PDG.

It is also necessary to consider the response speed of the negative feedback optical amplifier. A failure in superposition of the signal light and the return light without time delay will result in underutilization of the negative amplification effect or even in an adverse effect. SOA cross-gain modulation is in its principle of operation equivalent to the modulation of a probe light by a signal light. In the signal light input state (with level 0 changed to level 1), the induced emission is the main factor in the negative amplification feedback effect. In the change to the signal light non-input state (with level 1 changed to level 0), however, the spontaneous return of carrier density to the original level becomes the governing factor, and the feedback effect is influenced by the degree of relaxation at approximately 100 ps or higher. For high-speed cross-gain modulation, it is therefore essential to ensure high-speed carrier recovery. The effect of the FBG for negative feedback optical amplification was

demonstrated in the present study, but this effect cannot be expected if the input light signal and the negative feedback light signal do not superpose in time. In the prototype fabricated for this study, the separation between the SOA and the FBG was 1 mm or less. Calculations based on the results of this study indicate that, so long as a degree of signal superposition of about 90% can be assumed, the negative feedback effect can be maintained at up to about 10 Gbps, but further investigation will be necessary in this regard.

The present study included an investigation of the dependence of the BER and NF on the wavelength of the input signal. As indicated by Fig. 12, the SOA gain was shown to be wavelength dependent. Because of its origin in spontaneous emission, in contrast, the intensity of the negative feedback light returned by the FBG is independent of the input signal wavelength and it can therefore be considered essentially constant. The intensity of the negative feedback light acting on the input signal determines the degree of negative feedback amplification. The effect of the negative feedback light amplification will therefore be relatively small for input light signals of high-gain wavelength. As shown by the characteristics in Fig. 12 and Tables 1 and 2, an input light signal of 1530 nm showed high gain and the output light signal at that frequency was thus of higher intensity than at the other wavelengths. As the intensity of the negative feedback light returned by the FBG was essentially constant, it is apparently for this reason that the negative feedback light amplification effect was smaller for an input signal of that wavelength than for the other wavelengths of 1544, 1550, and 1558 nm, and the noise reduction effect was accordingly smaller. Conversely, the noise reduction effect was apparently larger with input signals of 1550 and 1558 nm, for which the SOA gain was relatively small, than with the other wavelengths because of the relatively strong negative feedback amplification effect for light of those wavelengths. The results of the measurements also showed the BER and NF to be smaller for the input signal of 1550 nm, which was the FBG center wavelength, than for the input signal of 1558 nm. This may be an effect of the dependence of the speed of propagation through the medium on the wavelength of the light reflected by the FBG. One further aspect which should be noted is the effect of the feedback on the output signal strength, as the measurements showed that the achievement of low noise with the negative feedback light was accompanied by a somewhat lower output (i.e., a somewhat lower degree of amplification). Among the FBG guidelines for practical applications, it will therefore be essential to ensure that the required output will be maintained while obtaining the required negative feedback effect.

In the present study, we have shown that it is possible to achieve negative feedback optical amplification by dynamic SOA gain modulation in correspondence with the input signal. Dynamic gain modulation is obtained by SOA cross-gain modulation, with effective utilization of the spontaneous emission within the SOA. It was shown, moreover, that this can be achieved with a simple, readily fabricated structure consisting of an optical fiber bearing written-in FBGs in addition to the SOA, which is highly advantageous for industrial applications. The results demonstrated, moreover, that by utilizing the NF-SOA it is possible to resolve otherwise intractable problems relating to SOA polarization dependence and noise characteristics. It is therefore expected that the proposed negative optical amplifier will find applications in many areas of optoelectronics, and it is believed that the proposal of this technique as one means of achieving an optical version of feedback amplification technology may be of major significance.

All-optical signal processing is expected to have a wide application in the field of communication and computation due to its capability of handling large bandwidth signals

and large information flows. Basic functions such as demultiplexing and switching can be achieved using all optical gates realized by optical nonlinearities in semiconductor materials. For future applications based on all-optical signal processing such as an optical computer, it will be very important to have optical devices showing the same functionality as transistors or triodes in electronics, including the capability of signal amplification. For the triode (i.e. three element tube), small voltage variations on the control grid produce large changes in plate current and voltage.

The proposed scheme shows several features that will be useful for the triode operation. Firstly the transmission gain of the device is directly controlled by the control beam power. Secondly it requires a small control power. The third advantage is that it shows optical signal amplification, which is very important for the cascadability of such devices. Finally, our setup is also flexible regarding the choice of the output wavelength, because we can either use the same wavelength as the input (as done here) or use a different one. Utilizing the advantages mentioned above, the all-optical triode has the potential to be the basis for logic gates and operational amplifiers in digital and analog optoelectronic circuits. This is in analogy with electronics, where devices like the transistors and triodes are the basis of logical gates and operational amplifiers. It is important to note that for the first time the principle of the all-optical triode based on SOAs is demonstrated. At the moment, the proposed scheme has some drawbacks in terms of speed and setup simplicity as compared to the integrated semiconductor devices (e.g. Mach-Zehnder interferometers). To be a practical viable solution to perform all-optical logic gate operation, our approach needs further improvements in terms of speed (for instance by using faster SOAs based on quantum dots).

6. Conclusion

In this study, a FBG for use as a negative feedback optical amplifier was produced by imprinting using the phase mask interference technique, which as a production method combines the high reproducibility of the phase mask technique and the wide wavelength range of the two-beam interference technique. The functions required of the FBG were that it transmit the wavelength of the input light injected into the SOA and simultaneously feed back to the SOA a part of the surrounding light generated in the amplification process. For this purpose, two chirp gratings with slightly different reflection center wavelengths were written onto the optical fiber in close proximity to each other. The use of the phase mask interference technique facilitated selection and control of the center wavelength, adjustment of the fiber write-in positions, and other process functions. The prototype FBG tip was lensed and coupled to one end of the SOA, thus forming a negative feedback semiconductor optical amplifier. In measurement of the bit error rate with a 10 Gbps pseudorandom signal with a wavelength of 1550 nm, which was the same as the FBG transmission center wavelength, the NF-SOA yielded an eye pattern with a higher aperture than those obtained at other frequencies. The BER curves obtained from the measurement results showed that the reduction in BER by the NF-SOA was clearly greater at 1550 nm than at the other wavelengths. At that wavelength, it resulted in a reduction of the noise figure to 5.1 dB. Based on these experimental findings, it was shown possible to reduce optical amplification noise to a low level with a NF-SOA using the FBG.

We also demonstrated an all-optical triode based on a tandem wavelength converter in two NF-SOAs using the same wavelength of input, control and output. This fact can be

important for logic applications. The all-optical triode has the input-output transfer function that is similar to the plate voltage-current characteristic of the triode in electronics including the signal amplification function. Because of its characteristics this device can become a key component in future all-optical signal processing and promote the realization of an optical computer.

7. Acknowledgement

This work was supported in part by the Ministry of Education, Culture, Science and Technology of Japan, a Grant-in-Aid （21560048）for Scientific Research (C).

8. References

Maeda, Y.; Tanimoto, H.; Matsuo, T.; Takagi, M. & Nakayama, H. (2010). "Noize reduction effect of negative feedback semiconductor optical amplifiers using fiber Bragg grating based on phase mask interferometer", *Rev. of Laser Engineering*, Vol.38, No.3, pp.219–224.

Maeda, Y. (2006). "Negative feedback optical amplification effect based on cross-gain modulation in semiconductor optical amplifier" *Appl. Phys. Lett.*, Vol.88, No.10, pp.101108-1 – 101108-3.

Maeda, Y. & Occhi L. (2003). "All-optical triode based on a tandem wavelength converter using reflective semiconductor optical amplifiers", *IEEE Photon. Technol. Lett.*, Vol.15, No.2, pp.257-259.

Bachmann, M.; Doussiere, P.; Emery, J. Y.; N'Go, R.; Pommereau, F.; Goldstein, L.; Soulage, G. & Jourdan, A. (1996). "Polarisation-insensitive clamped-gain SOA with integrated spot-size convertor and DBR gratings for WDM applications at 1.55μm wavelength", *Electron. Lett.*, Vol.32, No.22 pp.2076-2078.

Qureshi, K. K.; Tam, H. Y.; Lu, C. & Wai, P. K. A. (2007). "Gain control of semiconductor optical amplifier using a bandpass filter in a feedback loop", *IEEE Photon. Technol. Lett.*, Vol.19, No.18, pp.1401-1403.

Stubkjaer, K. E. (2000). "Semiconductor optical amplifier-based all-optical gates for high-speed optical processing", *IEEE J. Quantum Electron.*, Vol. 6, No. 6, pp. 1428-1435.

Glance, B.; Wiesenfield, J. M.; Koren, U.; Gnauck, A. H.; Presby, H. M. & Jourdan, A. (1992). "High performance optical wavelength shifter", *Electron. Lett.*, Vol.28, No.18, pp.1714-1715.

Wiesenfeld, J. M. (1996). "Gain dynamics and associated nonlinearities in semiconductor optical amplifiers", *J. High speed electronics and systems*, Vol.7, No.1, pp.179-222.

Durhuus, T.; Joergensen, C.; Mikkelsen, B.; Pedersen, R. J. S. & Stubkjaer, K. E. (1994). "All optical wavelength conversion by SOAs in a Mach-Zehnder configuration", *IEEE Photon. Technol. Lett.*, Vol. 6, pp.53-55.

Sun, J. (2003). "Theoretical study on cross-gain modulation wavelength conversion with converted signal feedback"*IEE Proc. Optoelectron.*, Vol. 150, No.6, pp.497-502.

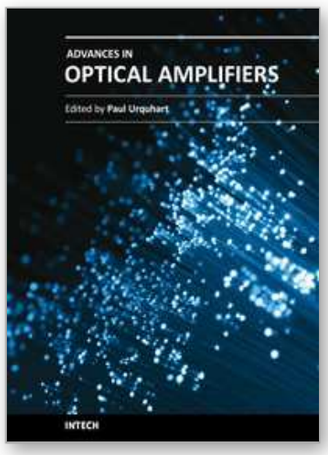

Advances in Optical Amplifiers
Edited by Prof. Paul Urquhart

ISBN 978-953-307-186-2
Hard cover, 436 pages
Publisher InTech
Published online 14, February, 2011
Published in print edition February, 2011

Optical amplifiers play a central role in all categories of fibre communications systems and networks. By compensating for the losses exerted by the transmission medium and the components through which the signals pass, they reduce the need for expensive and slow optical-electrical-optical conversion. The photonic gain media, which are normally based on glass- or semiconductor-based waveguides, can amplify many high speed wavelength division multiplexed channels simultaneously. Recent research has also concentrated on wavelength conversion, switching, demultiplexing in the time domain and other enhanced functions. Advances in Optical Amplifiers presents up to date results on amplifier performance, along with explanations of their relevance, from leading researchers in the field. Its chapters cover amplifiers based on rare earth doped fibres and waveguides, stimulated Raman scattering, nonlinear parametric processes and semiconductor media. Wavelength conversion and other enhanced signal processing functions are also considered in depth. This book is targeted at research, development and design engineers from teams in manufacturing industry, academia and telecommunications service operators.

INTECH
open science | open minds

InTech Europe
University Campus STeP Ri
Slavka Krautzeka 83/A
51000 Rijeka, Croatia
Phone: +385 (51) 770 447
Fax: +385 (51) 686 166
www.intechopen.com

InTech China
Unit 405, Office Block, Hotel Equatorial Shanghai
No.65, Yan An Road (West), Shanghai, 200040, China
中国上海市延安西路65号上海国际贵都大饭店办公楼405单元
Phone: +86-21-62489820
Fax: +86-21-62489821

IntechOpen